doi: 10.5028/jatm.2012.04032912

Bonded Joints Design Aided by Computational Tool

Marcelo L. Ribeiro*, Volnei Tita
Escola de Engenharia de São Carlos/Universidade de São Paulo – São Carlos/SP- Brazil

Abstract: *In order to aid the design of bonded joints, a computational tool named System of Analysis for Joints (SAJ) was developed. The software can analyze single and double lap bonded joint with composite-composite or metal-composite materials as adherent parts. Thus, SAJ can calculate the stress distribution, loads and displacements. Their results were compared to finite element software (ABAQUS™) and to specific composite analysis software (ESAComp™). After that, a study about the influence of joint design parameters on the mechanical behavior of the bonded joint was carried out. In regards to parametric study, SAJ leads to some conclusions, which can be used as a guide during the product design process. Therefore, aided by the computational tool, it is possible to perform a conceptual and preliminary design of bonded joints with more accuracy and varying many parameters (materials; fiber orientation and stacking sequence of the laminate; thickness; overlap length).*

Keywords: *Bonded joints, Design parameters, Composite joints, Computational tool, Adhesives, Stress analysis.*

LIST OF SYMBOLS

a_{ij}^{k}	Membrane compliance term for composite adherent *k, k* =1,2,3
b_{ij}^{k}	Coupling compliance term for composite adherent *k, k* =1,2,3
d_{ij}^{k}	Bending-torsion compliance term for composite adherent *k, k* =1,2,3
E_1	Young modulus in fiber direction
E_2	Young modulus in transverse direction of the fiber
G_{12}	Shear modulus in ply plane
E_a	Adhesive young modulus
G_a	Adhesive shear modulus
u_0^i	Middle plane adherent displacement in *x* direction for adherent *i, i* =1,2,3
v_0^i	Middle plane adherent displacement in *y* direction for adherent *i, i* =1,2,3
w^i	Adherent displacement in *z* direction for adherent *i, i* =1,2,3
N_x^i	Normal force in *x* direction for adherent *i, i* =1,2,3
N_y^i	Normal force in *y* direction for adherent *i, i* =1,2,3
Q_x^i	Shear force in the x-face of infinitesimal element for adherent *i, i* =1,2,3
Q_y^i	Shear force in the y-face of infinitesimal element for adherent *i, i* =1,2,3
M_{xx}^i	Moment around *x* axis for adherent *i, i* =1,2,3
M_{yy}^i	Moment around *y* axis for adherent *i, i* =1,2,3
M_{xy}^i	Moment around *y* axis in the *x* face of infinitesimal element for adherent *i, i* =1,2,3
M_{yx}^i	Moment around *x* axis in the *y* face of infinitesimal element for adherent *i, i* =1,2,3
t_i	Thickness of the adherent *i, i* =1,2,3
t_{ai}	Thickness of the adhesive layer *i, i* =1,2
σ_{azj}	Normal stress in adhesive layer in *z* direction for adhesive *j, j* =1,2
τ_{axj}	Shear stress in adhesive layer in *xz* plane for adhesive *j, j* =1,2
τ_{ayj}	Shear stress in adhesive layer in *yz* plane for adhesive *j, j* =1,2
υ	Poisson's coefficient

Received: 15/05/12 Accepted: 02/07/12

*author for correspondence: malribei@usp.br
Department of Aeronautical Engineering – EESC/USP, Av. João Dagnone, 1100 – Jardim Santa Angelin CEP 13563-120, São Carlos – SP/Brazil

INTRODUCTION

In the last years, the usage of composite materials as a primary structural element has increased. Some new aircraft designs, such as Airbus A380 and Boeing 787, use composite materials even for primary structural elements, such as wing spars and fuselage skins, achieving lighter structures without reducing of airworthiness. One way to assemble those parts is to apply a bonded joint, which possesses some advantages, for

example: better fatigue endurance; joining dissimilar materials; better insulation; smooth surface and lower weight. However, there are also negative aspects, for example: no possibility to disassemble the joints; peeling stress should be minimized and the preparation of the surfaces for bonding must be done carefully (Mortensen, 1998). Besides, it is very difficult to predict the stress distribution in bonded joints and many design parameters influence the mechanical behavior of this type of joint.

Regarding this scenario, many researchers have conducted studies about bonded joints, trying to predict their mechanical behavior by finite element models, analytical models, experimental tests or hybrid approaches, combining theoretical and experimental analyses. The first analyses for bonded joints were carried out by Volkersen in 1938 (Mortensen, 1998). Volkersen modeled the adhesive layer as shear spring distributed over the double lap joint, disregarding the flexural effects (Mortensen, 1998). The results obtained by the researcher showed that the load transfer at the adhesive was not uniform. Goland and Reissner (1944) improved Volkersen's model by considering the adherent like beams and the adhesive like springs in tension and shear loading. That model could analyze the distribution of the transversal loading induced by the secondary moment, which occurs in single lap joints. Hart-Smith (1970; 1973), based on the last models, introduced the influence of the thermal expansion between the materials. Hart-Smith simulated the adhesive response, using an elastic-plastic material model. It is important to mention that Hart-Smith (1970; 1973) investigated the influence of the main design parameters in the structural performance of the joint too. However, some of those models assumed that the laminates were isotropic or symmetric (only with tension and flexural stiffness), disregarding the layers and considering apparent properties for the laminates. In 1975, Yuceoglu and Updike improved Hart-Smith's model by considering the transversal shear effects in the adherent. They showed that if the adherents have strong anisotropy and higher flexibility in shear loading, the normal strains can affect the stress distribution in the adhesive. Thomsen (1992) showed that an increase in the overlap length reduces the stress level in the adhesive layer. The researcher concluded that the application of adhesive layer with lower elastic shear and tensile moduli decreases the adhesive stress. Thomsen (1992) verified that it is better to use identical or nearly identical adherents in bonded joints, i.e., adherents with similar stiffness. Frostig *et al*. (1998) proposed an approach using high-order theory. In their analysis, the adhesive was modeled as an elastic continuum media (2D and 3D). So, the adhesive could transfer normal stresses, in-plane and transversal shear stresses. These results showed that there was a great variation of the normal stress in the adhesive close to the edges.

Springer and Ahn (1998) modified Hart-Smith's model applying the Classical Laminate Theory (CLT). For the initial analyses, the adhesive layer was considered as homogeneous, isotropic and linearly elastic, but the adhesives used at aeronautical industry have non-linear behavior. Thus, for the follow-up analyses, the Springer and Ahn's model considered the elastic-plastic response for the adhesives (Springer and Ahn, 1998). Mortensen (1998), in his Ph.D. thesis, presented a development of a computational tool for analysis of bonded joints, showing the equations and hypothesis for various types of joints. The author showed the solving process of differential equations, using the multi-segment method of integration. Four years later, Ganesh and Choo (2002) showed the effect of spatial grading of adherent elastic modulus on the peak of stress and stress distribution in the single lap joint. This effect decreases the stress peak and provides a more uniform shear stress distribution in the joint. After that, Belhouari *et al*. (2004) showed a comparison between single and double lap joint using a finite element model. In that study, the researchers showed the advantages of using a symmetric composite patch in order to repair the damage parts; also, that double patch had lower stress when compared with single patch repair. Regarding the manufacturing process parameters, Seong *et al*. (2008) showed that an increase of bonding pressure during the manufacturing process leads to higher strength bonded joints. The researchers verified that an increase in the overlap length also leads to higher strength bonded joints, and the major failure mode for single lap composite-aluminum joints is the delamination of the composite adherent. In the same year, based on experimental analyses, Kim *et al*. (2008) investigated the influence of the overlap length and observed that the normal and shear stresses at the adhesive region reduce when the overlap increases.

However, it is important to mention that other researchers preferred to analyze bonded joints by the Finite Element Method, for example: Charalambides *et al*. (1998); Goyal *et al*. (2008). Besides, some researchers compared analytical methods to numerical approaches. Zarpelon (2008) carried out a comparison between Mortensen's model and finite element analyses to evaluate the mechanical behavior of single and stepped joints. Zarpelon concluded that Mortensen's model produces good results for symmetric laminates, but for laminates with higher asymmetry, the model should be improved. In fact, Mortensen's model assumes cylindrical flexural hypothesis, which is not adequate to simulate the laminates

with warping effects. Agnieszka (2009) showed a numerical method, regarding the sensitivity to hydrostatic stress for prediction of the delamination initiation. This method allows simulating the failure in the joint (at the overlap region) and in the adherent. Silva *et al*. (2009a; 2009b) showed an excellent bibliographic review about models for bonded joints and performed a comparison between the most important models, showing the advantages and limitations for each one. More recently, Xiaocong (2011) showed a review about finite element method applied to simulate bonded joints.

In many studies commented earlier, the researches proved that different design parameters can influence the mechanical behavior of bonded joints due to the interaction phenomena (for example: mechanical, physical and chemical interactions) between parts (adherents) and adhesives. Besides, the type of the fiber and the matrix of the composite, as well as the stacking sequence of the laminate can change the structural performance of the bonded joints. Therefore, it can be concluded that the design and analysis of bonded joints is very complex problem, which there is not still a closed solution. Thus, new proposals to solve this problem are required.

In order to aid the design of bonded joints, a computational tool named System of Analysis for Joints (SAJ) was developed, which is capable of analyzing not only single lap joint, but also double lap joint. These joints could be made of composite-composite materials or dissimilar materials, i.e., metal-composite. For both types of joints, SAJ can calculate the stress and strain distributions, loads and displacements. In order to evaluate the limitations and advantages of the SAJ, some analyses were performed, using case studies. Moreover the SAJ results were compared to finite element software (ABAQUS™) and to specific composite analysis software (ESAComp™). After that, a study about the influence of bonded joint design parameters on its mechanical behavior was carried out (overlap length; type of joint; adhesive elastic modulus and adhesive layer thickness).

THE COMPUTATIONAL TOOL – SAJ

The computational tool was developed to calculate the joint loads, displacements and adhesive/adherents stresses with non-linear effects (Ribeiro *et al.*, 2010). This computational tool named SAJ was programmed in Matlab™ language and can analyze single and double lap bonded joints. In fact, SAJ can predict the mechanical behavior of composite-composite and metal-composite bonded joints. Regarding composite adherents, the computational tool can calculate the stress and strain distributions in each layer of the laminate.

To predict the mechanical behavior of bonded joints, SAJ reads an input file with data of adherents, adhesive and joint characteristics. This file contains information such as layup and layer thickness in case of composite adherents, mechanical properties for adherents and adhesives, joint dimensions of adhesive and adherents, as well as loads and boundary conditions. Using the input data, SAJ builds a set of differential equations, which is solved by Matlab™. After that, SAJ shows forces, displacements and adhesive stresses by graphics and tabular format.

Mathematical formulation

A set of differential equations of the multi-domain boundary value problem is implemented in SAJ. In order to obtain this set of differential equations, the problem domain (bonded joint) is partitioned in three regions: one part for adherents only, other part for the bonded region (overlap region) and the last part, again, only for adherents. Figure 1 shows these subdivisions, coordinate system, as well as an example of boundary conditions and loads for single lap joint (Fig. 1a) and double lap joint (Fig. 1b).

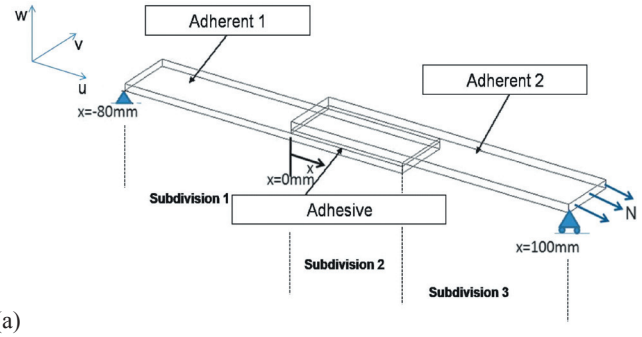

(a)

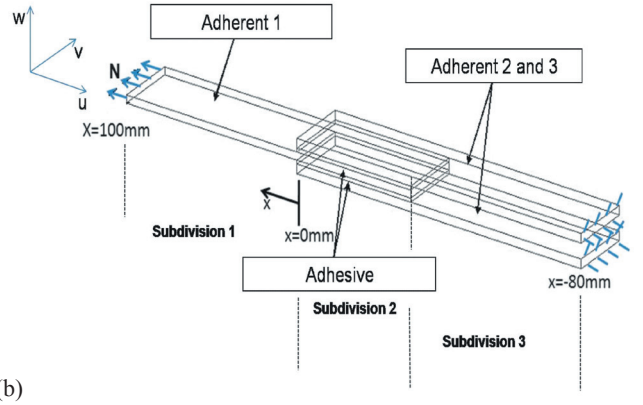

(b)

Figure 1. Boundary conditions, loads and coordinate system: (a) single lap joint; (a) double lap joint.

For each region, free body diagrams of equilibrium in an infinitesimal volume element can be obtained as shown in Fig. 2. Thus, the set of differential equilibrium equations for single and double lap joints can be written. Based on these equations and applying the hypothesis that all derivatives in y direction are equal to zero (cylindrical bending hypothesis), as well as considering plane stress state and Kirchhoff's kinematic relations, it is possible to obtain the set of differential equations shown by Fig. 2 For composite adherents, some terms of the equations are calculated using the CLT and the symbols a_{ij}, b_{ij} and d_{ij} at Fig. 2 correspond to components of laminate compliance matrix. The membrane, coupling and bending-torsion compliances are represented by a_{ij}, b_{ij} and d_{ij}, respectively. Also, at the Fig. 3, the sub index comma with "x" means partial derivate in "x".

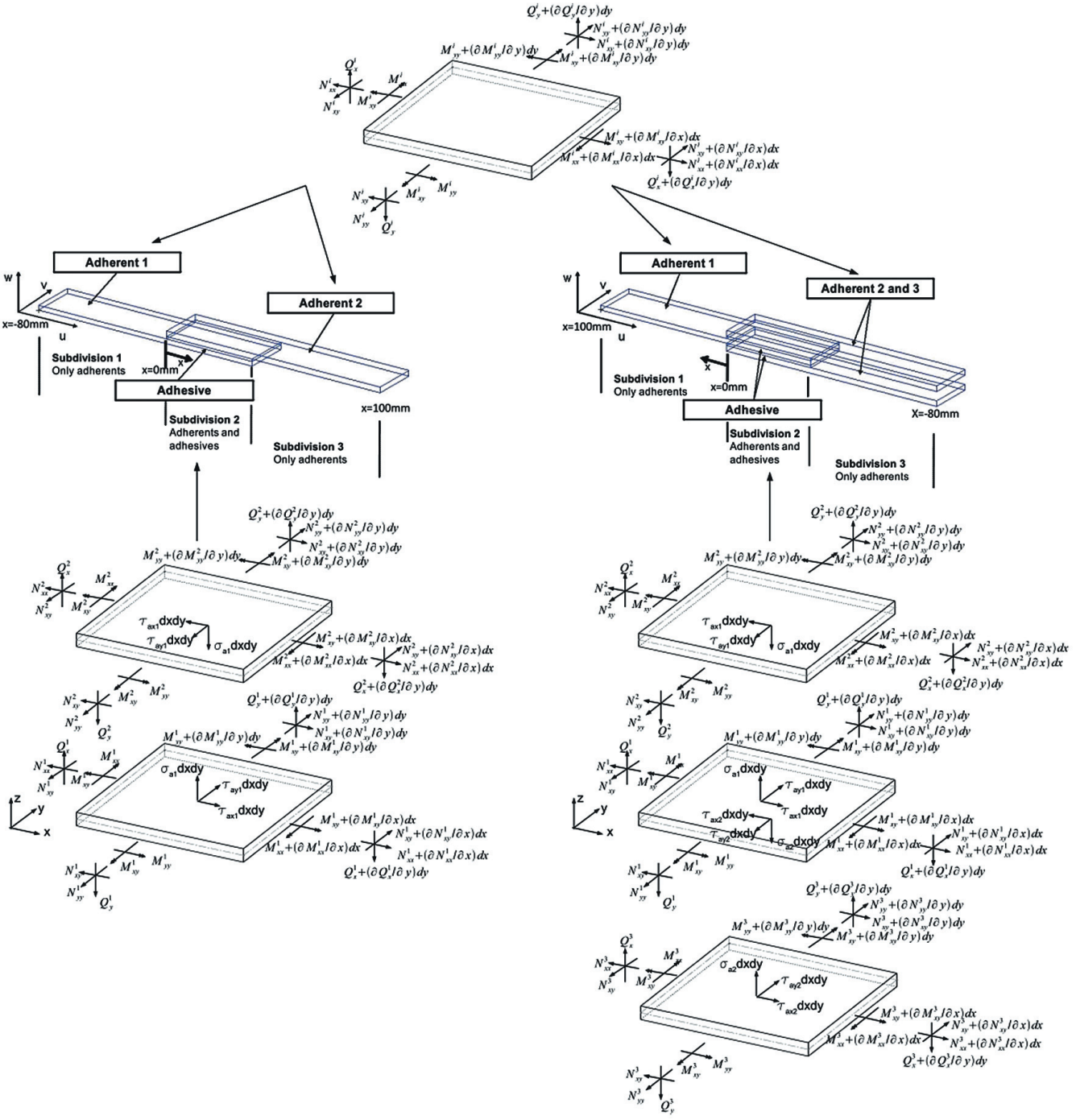

Figure 2. Free body diagrams for equilibrium forces in each subdivision part.

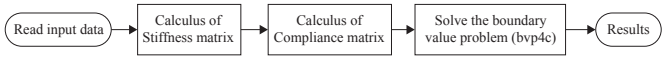

Figure 3. General flow chart of System of Analysis for Joints.

Using the free-body diagrams (Fig. 2) and CLT, the set of equations for the subdivisions out of overlap region (single or double lap joint) is presented in Eq. 1. The upper letter *i* ($i = 1, 2, 3$) indicates the adherent.

$$\begin{aligned}
&u^i_{0,x} - a^i_{11}N^i_{xx} - a^i_{13}N^i_{xy} - b^i_{11}M^i_{xx} = 0\\
&w^i_{,xx} + k^i_x = 0\\
&k^i_x - b^i_{11}N^i_{xx} - b^i_{13}N^i_{xy} - d^i_{11}M^i_{xx} = 0\\
&v^i_{0,x} - a^i_{21}N^i_{xx} - a^i_{23}N^i_{xy} - b^i_{21}M^i_{xx} = 0\\
&N^i_{xx,x} = 0\\
&N^i_{xy,x} = 0\\
&M^i_{xx,x} = 0\\
&Q^i_{x,x} = 0
\end{aligned} \tag{1}$$

Regarding the double lap joint, the same procedure described before (free-body diagrams and CLT) is used to obtain the set of differential equations for double lap joint adherent 1 (Fig. 2). Equation 2 shows the set of differential equations for this region.

$$\begin{aligned}
&u^1_{0,x} - a^1_{11}N^1_{xx} - a^1_{13}N^1_{xy} - b^1_{11}M^1_{xx} = 0\\
&w^1_{,xx} + k^1_x = 0\\
&k^1_x - b^1_{11}N^1_{xx} - b^1_{13}N^1_{xy} - d^1_{11}M^1_{xx} = 0\\
&v^1_{0,x} - a^1_{21}N^1_{xx} - a^1_{23}N^1_{xy} - b^1_{21}M^1_{xx} = 0\\
&N^1_{xx,x} + \tau_{ax1} - \tau_{ax2} = 0\\
&N^1_{xy,x} + \tau_{ay1} - \tau_{ay2} = 0\\
&M^1_{xx,x} - Q^1_x + \tau_{ax1}\frac{(t_1 + t_{a1})}{2} - \tau_{ax2}\frac{(t_1 + t_{a2})}{2} = 0\\
&Q^1_{x,x} - \sigma_{az1} + \sigma_{az2} = 0
\end{aligned} \tag{2}$$

For the other regions in the overlap area (double and single lap joint), the resulting set of differential equations is presented in Eq. 3. In this case, the upper letter i ($i = 1, 2$) indicates the adherent for single lap joint or *i* ($i = 2, 3$) indicates the adherent for double lap joint.

$$\begin{aligned}
&u^i_{0,x} - a^i_{11}N^i_{xx} - a^i_{13}N^i_{xy} - b^i_{11}M^i_{xx} = 0\\
&w^i_{,xx} + k^i_x = 0\\
&k^i_x - b^i_{11}N^i_{xx} - b^i_{13}N^i_{xy} - d^i_{11}M^i_{xx} = 0\\
&v^i_{0,x} - a^i_{21}N^i_{xx} - a^i_{23}N^i_{xy} - b^i_{21}M^i_{xx} = 0\\
&N^i_{xx,x} + \tau_{ax} = 0\\
&N^i_{xy,x} + \tau_{ay} = 0\\
&M^i_{xx,x} - Q^i_x + \tau_{ax}\frac{(t_1 + t_a)}{2} = 0\\
&Q^i_{x,x} - \sigma_{az} = 0
\end{aligned} \tag{3}$$

It is important to mention that the adhesive is simulated as springs under tension or compression combined to shear stresses as shown by the following equations:

$$\tau_{ax} = \frac{G_a}{t_a}\left(u^i_0 - \frac{t_i(x)}{2}\cdot k^i_x - u^{i+1}_0 - \frac{t_{i+1}(x)}{2}\cdot k^{i+1}_x\right) \tag{4}$$

$$\tau_{ay} = \frac{G_a}{t_a}(v^i_0 - v^{i+1}_0) \tag{5}$$

$$\sigma_{az} = \frac{E_a}{t_a}(w^i - w^{i+1}) \tag{6}$$

where t_i is the thickness of the *i* adherent ($i = 1, 2, 3$), t_a is the adhesive thickness, κ_x is the rotation at the *x* axis, u_0 is the middle plane displacement in *x* direction and v_0 is the middle plane displacement in y direction.

Regarding the boundary conditions, in general they are provided as forces, moments or displacements in the edges of the problem domain which will be described in more detail in the following sections.

Finally, the differential equations for each subdivision are solved using Matlab™, which can deal with multi-domain boundary value problem, also each subdivision are divided in n parts (mesh). It is important to mention that the ESAComp™ has basically the same formulation used in SAJ, but the solving process is different.

Numerical analyses procedure

The numerical analysis starts after SAJ reads input data from a file, which prescribe the joint type (single or double), adherents and adhesives mechanical properties, ply thickness and orientation (in case of composite materials), adhesive thickness and the dimensions, as well as loads and boundary conditions. Based on these data, SAJ calculates the stiffness and the compliance matrix. For composite parts (adherents), the CLT is applied.

Knowing the joint type, the boundary conditions and the compliance matrix calculated in a previous step, SAJ builds the set of differential equations presented earlier. This set of equations comprises on a boundary value problem, which is solved by "bvp4c" Matlab™ function. After that, SAJ shows the results by graphics and tabular format (Fig. 3).

For a better understanding of the differences between the numerical methods used, a short description of multiple point shooting method used by ESAComp™ and the Matlab™ function "bvp4c" are shown later. The finite element method is assumed to be well-known by the readers.

Multiple point segment method (ESAComp™)

Multiple point segment method is used for the boundary value problem with several initial conditions. In this method the domain is subdivided in *n* parts.

This method starts with an approximation for the equation derivative in one side of the domain ($x = 0$) regardless the value in the other side ($x = 1$) (Fig. 4). Moreover, this method uses the fourth order Range-Kutta (Butcher, 2003) to solve the set of differential equations 1 to 3.

With the initial shoot for the derivative in $x = 0$ the solution of the set of differential equations in $x = 1$ is compared with the prescribed value in this position. If the value of the numerical solution is not the right value (regarding specified tolerance), other approximation for the derivative in $x = 0$ is used. This procedure is repeated until the solution converges to the desired value.

The multiple point segment method requires low computational cost; on the other hand, this method only works for simple problems (Saha and Banu, 2007). More details can be seen in Appendix I.

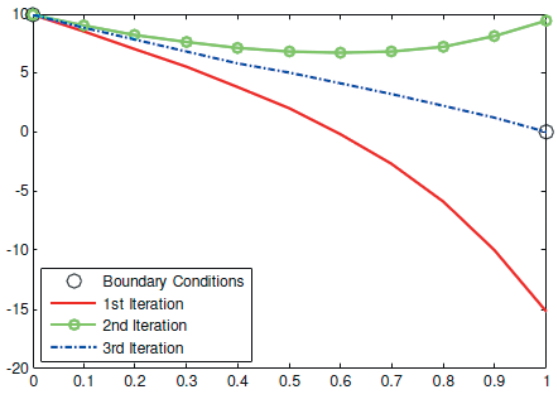

Figure 4. Solution of the boundary value problem using multiple point segment method. *x*-axis: problem domain; *y*-axis: possible solutions

Matlab "bvp4c" function

The Matlab function "bvp4c" is the Simpson method to solve boundary value problem. Shampine *et al.* (2006) described how this method can solve the boundary value problem (see Appendix II for more detail).

The difference between the multipoint segment method, that is a shooting method, and the "bvp4c" function are that the solutions $y(x)$ are approximated for the entire interval and the boundary conditions are considered every time during the solution. This method requires a discretization of the domain as well as for finite element method.

RESULTS AND DISCUSSIONS

Evaluation of the computational tool (SAJ)

A finite element model for single and double lap joint using commercial software ABAQUS™ was developed to compare the results to the SAJ analyses. The finite element model (single and double lap joint) uses a second-order hexahedron element with 20 nodes (C3D20) for adherents, the adhesives were modeled with a second-order hexahedron element with 20 nodes (C3D20) too. ABAQUS™ constraint function "tie" is used to join the adhesive and adherents in the overlap region. This constraint function transfers all degrees of freedom between adherents and adhesive. Figure 5a shows the finite element model for single lap bonded joint and Fig. 5b shows the finite element model for double lap bonded joint.

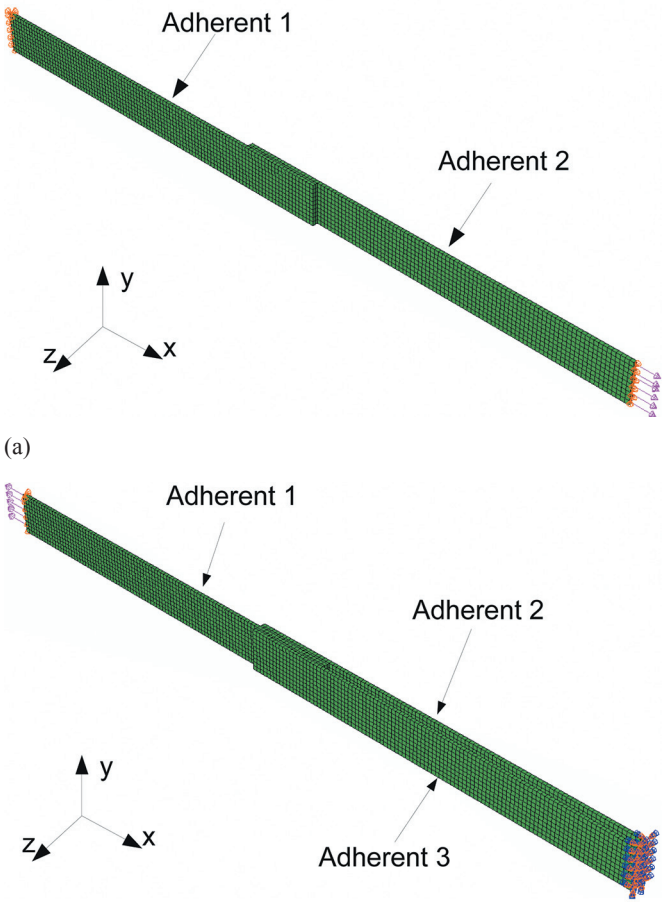

Figure 5. Finite element model: (a) single lap joint; (b) double lap joint.

For the first set of analyses, symmetric laminate composite-composite single and double lap bonded joints were investigated. The adherent and adhesive mechanical properties and the joint characteristics are shown in Table 1. A normal load in x direction of 1 N/mm was applied on single and double lap joint. This load is small enough in order to avoid inelastic strains in adherents or in adhesive. Also, all the stresses in the adhesive layer will be divided by the applied stress (normalized stresses) in order to improve the comprehension of the load transfer by the bonded joint.

Figure 6a shows the displacement field in z direction for single lap joint. It is possible to verify the difference between results from SAJ and from other software. For the finite element model, at the edge of adherent 1, all displacements (x, y and z) are fixed and all rotations are free (Fig. 5a). In the opposite edge, at adherent 2, z displacement is fixed, all

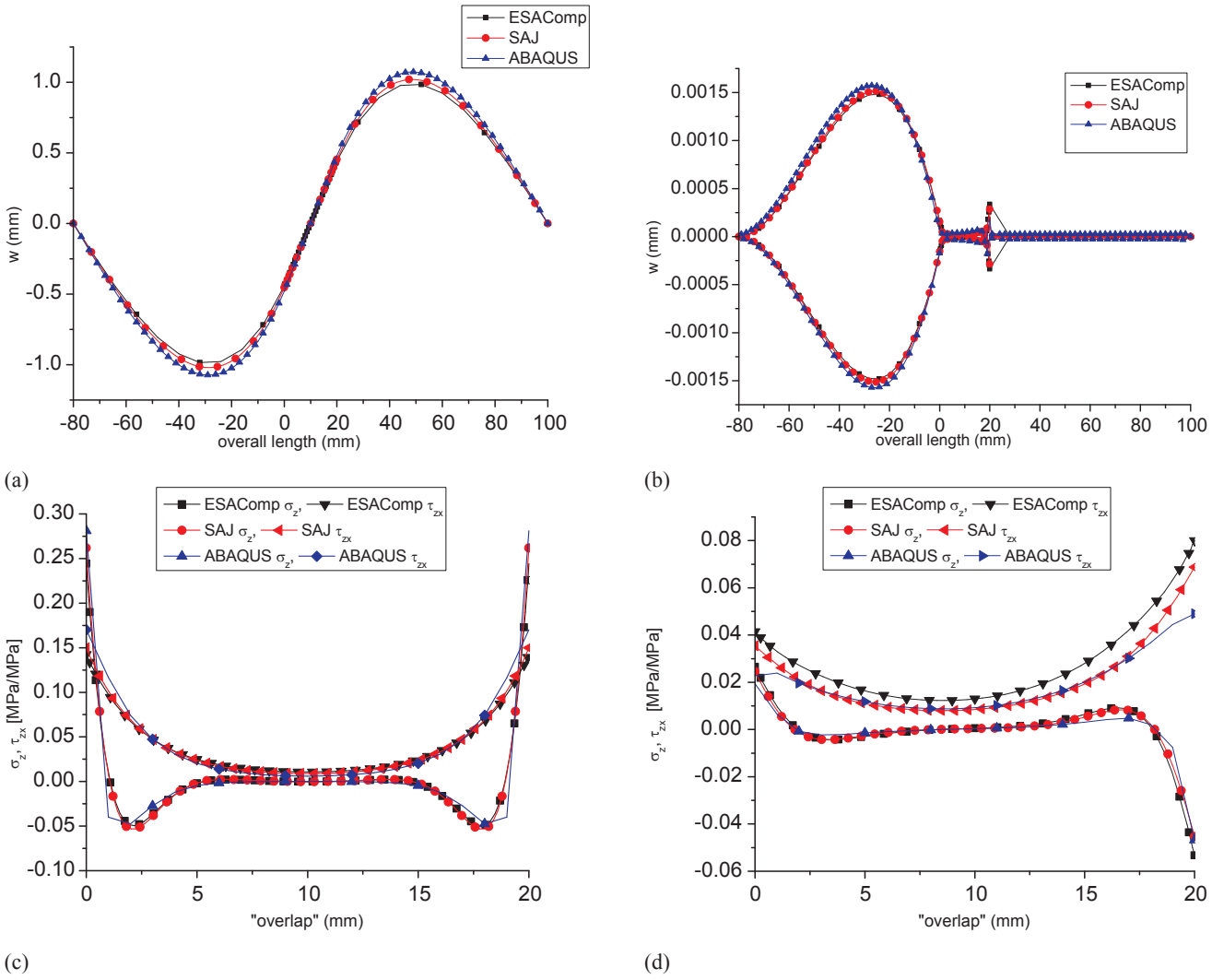

Figure 6. (a) Single lap composite joint displacement in $w(z)$ direction; (b) double lap composite joint displacement in $w(z)$ direction; (c) normalized single lap joint σ_{az} and τ_{ax} ; (d) normalized double lap joint σ_{az} and τ_{ax}.

Table 1. Mechanical properties and joint characteristics: Hexcel T3T-190-F155/carbon fiber reinforced plastic, Hysol EA9321/epoxy adhesive and aluminum/2024-T3 (Tita *et al*., 2008)

	E_1 [kN/mm²]	E_2 [kN/mm²]	G_{12} [kN/mm²]	Y	Thickness [mm]	Orientation
Hexcel T3T-190-F155	126.0	7.1	4.0	0.3	0.8 (0.2mm per ply)	$[0/45]_s$
Epoxy adhesive	1.485	-	-	0.35	0.5	-
2024-T3	72.0	-	-	0.33	0.8	-

rotations are free and the loading is applied in x direction (Fig. 5a). For SAJ, at the edge of the adherent 1, $x(u)$ and $z(w)$ displacements are fixed and rotation at $y(v)$ is free (Fig. 1a). In the opposite edge, at adherent 2, z (w) displacement is fixed, rotation at y (v) is free and the normal loading is applied in *x(u)* direction (Fig. 1a).

The boundary conditions applied for finite element model and SAJ are almost the same. These small differences are due to limitations of the hypothesis adopted for SAJ and the mathematical procedure used to solve the set of differential equations. Thus, the displacement field of finite element model is a little bit higher than SAJ, i.e. the SAJ model is slightly stiffer than finite element model. Both SAJ and ESAComp™ do not regard for free edge effects on the adhesive layer.

It is important to mention that the commercial software ESAComp™ has some limitations of boundary conditions once only three types of boundary conditions are available. In fact, real structures boundary conditions are rather difficult to be simulated, thus simplifications must be assumed. Despite SAJ uses the same set of equations used in ESAComp™, this computational tool is more flexible to simulate different boundary conditions, but still has some limitations (for some boundary conditions was not possible to solve the set of differential equations). Despite the limitations to apply boundary conditions showed by ESAComp™ and SAJ, in the finite element model is possible to simulate any boundary conditions. So, in order to proceed with the analysis, the boundary conditions between SAJ and ESAComp™ were keep as close as possible as well as for the finite element model. The ESAComp™ boundary conditions are:

- Simple Supported (SS): in this condition in one edge all the displacements are restricted and in the other edge only the vertical displacement is restricted. All the moments are free;
- Clamped-Free (CF): in this boundary condition one edge is clamped (all displacements and rotations are restricted) and the other edge is completely free;
- Clamped-Clamped (CC): this condition means that one edge all the degrees of freedon are restricted and in the other edge only the rotations are restricted.

Due to ESAComp™ limitations, the boundary conditions used for simulations were similar to SS.

The differences between SAJ and ESAComp™ responses (Fig. 6) are due to numerical differences to solve the set of differential equations and small differences in the boundary conditions. Figure 6a shows the displacement field for the entire single lap joint. The joint dimensions and coordinates were shown in Fig. 1a for single lap joint and Fig. 1b for double lap joint.

Figure 6b shows the displacement field for the entire double lap joint and all results are very close. For the finite element model, in the edge of adherents 2 and 3, all displacements and rotations are fixed (Fig. 5b). In the opposite edge, at adherent 1, only the loading is applied in x direction (Fig. 5b). For SAJ, in the edge of the adherents 2 and 3, $x(u)$ and $z(w)$ displacements are fixed and all rotations are fixed (Fig. 1b). In the opposite edge, at adherent 1, only the normal loading is applied in $x(u)$ direction (Fig. 1b). The same consideration for boundary conditions is applied to this case. Thus, the displacement field of finite element model is a little bit higher than SAJ, i.e. the SAJ model is slightly stiffer than finite element model.

Regarding to ESAComp™, the CF boundary conditions were adopted which are, as for the last case, the most similar boundary conditions available in the software to proceed with the evaluations. In this case, despite the differences, the results are very close to SAJ (Fig. 6).

Figure 6c shows the normalized σ_{az} and τ_{ax} for single lap bonded joint and all results are again similar too. In this case, it is possible to observe that the normal stress in the adhesive layer σ_{az} has a relatively high tensile stress in the adhesive edge, than it changes to compressive stress in less than 2.5 mm and in 5.0 mm the normal stress is almost zero or has a very low value. The same behavior is observed in the other edge. Equation 6 explains this behavior (for SAJ and ESAComp™) once it regards the relative displacement between the adherents. The single lap joint finite element also has the same behavior for normal stress in the adhesive layer.

Figure 6d shows that SAJ results of σ_{az} and τ_{ax} for double lap joint converge on the finite element model results. However, the ESAComp™ results are different. These differences depend on the boundary conditions imposed by each software, as well as the solution algorithm used in each model. It is important to note that the highest differences are observed at the end of the overlap region, where the highest stress values are observed. The stress singularity is not observed for double lap joint.

For the second set of analyses, metal-composite single and double lap bonded joint were investigated. Again a normal load in x direction of 1 N/mm was applied on single and double lap joint. There is no change in the composite lay-up.

For single lap joint, aluminum was used for adherent 1 and composite laminate for adherent 2 (Fig. 1a). For double lap joint, aluminum was used for adherent 1 and composite laminates for adherents 2 and 3 (Fig. 1b). The material properties

are shown in Table 1. The boundary conditions and loading for single and double lap joints were applied as commented earlier.

Figure 7a shows the displacement field for the entire single lap joint, where ESAComp™ results are more flexible in the composite side and stiffer in the aluminum side. SAJ results are between ESAComp™ and finite element model results. This occurs due to differences in computational method applied to solve the problem, as well as the boundary conditions applied. Figure 7b shows the displacement field for the entire double lap joint and the SAJ results converge to the finite element results. However, the ESAComp™ results are different due to the applied boundary conditions. Figure 7c shows σ_{az} and τ_{ax} for single lap bonded joint and all results are very close. The stress singularity appears again for single lap hybrid joint.

For double lap joint, there are differences between the results of σ_{az} and τ_{ax} (Fig. 7d). These differences depend on the applied boundary conditions, as well as the solution algorithm used in each model, as discussed earlier. It is important to note, again, that the highest differences are observed at the end of the overlap region, where the highest stress values are verified. The results for SAJ and ESAComp™ are very similar, but the finite element model results show lower stress values. This occurs because SAJ and ESAComp™ use a cylindrical flexural hypothesis as described by Mortensen (1998).

As commented before, the stress singularity that appears for single lap joints (composite-composite or composite-metal) is due to the relative displacements between the adherents (Eq.6). Once the set of equations (Eqs. 2 and 3) regards the adhesive stresses they affect the solution and then in the adherents kinematics. In the single lap joint solution, inside the overlap

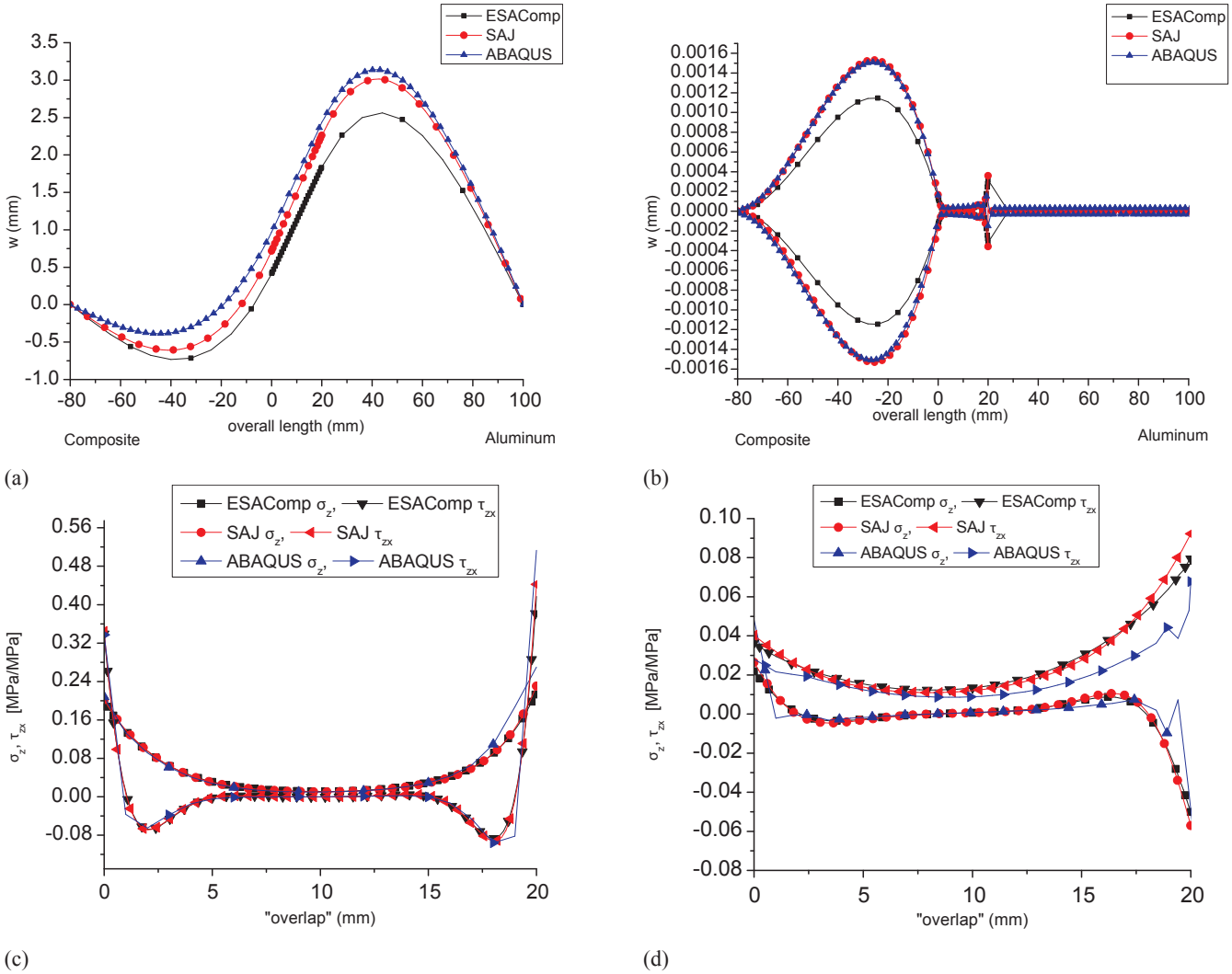

Figure 7. (a) Single lap hybrid joint displacement in w direction; (b) double lap hybrid joint displacement in w direction; (c) normalized single lap joint σ_{az} and τ_{ax}; (d) normalized double lap joint σ_{az} and τ_{ax}.

region, the w displacement of adherent 2 (see Eq. 6) becomes bigger (in absolute value) than the vertical displacement of adherent 1. This behavior leads to a compressive normal stress in the adhesive layer. Also it is important to mention that the numerical procedures used in SAJ or in ESAComp™ smooth the results between each subdivision avoiding discontinuity for the solution. The single lap finite element model also shows the same behavior for normal stress, confirming that the relative displacement between the adherents leads to a compressive normal stress close to the adhesive layer edges.

Considering the results shown earlier, it is possible to conclude that SAJ is a computational tool, which can predict the mechanical behavior of composite-composite and metal-composite bonded joints (single and double) with similar accuracy shown by other software. Therefore, in the next section, some design parameters will be investigated in order to study their influence on the structural performance of bonded joints.

Design parameters study for composite bonded joints using SAJ

One of the most important components of the joint is the adhesive layer at the overlap region, where physical and chemical interactions between adherents and adhesive occur and the load is transferred from the part (adherent) to the adhesive and vice versa. Thus, design parameters such as overlap length, type of joint, adhesive elastic modulus, and adhesive layer thickness, which affect the stress distribution in the overlap region, mainly the σ_{az} and τ_{ax} component stresses, were investigated. For all parametric studies, the boundary conditions and loading were applied as described here in section Evaluation of the computational tool (SAJ). The mechanical properties and other important characteristics for adhesive and adherents are given in Table 2 for both types of joints (single and double).

Effect of the overlap length

For this investigation, metal-composite single and double lap joints were used. A load of 1 N/mm was used for both types of joints. Aluminum 2024-T3 was assumed in single lap joint as adherent 1, and for adherent 2, carbon fiber composite (Hexcel T3T-190-F155). For the double lap joint, aluminum 2024-T3 was assumed for adherent 1, and composite material was applied for other adherents. An epoxy adhesive was considered for both types of joints.

Figure 8a shows the effect of the overlap length in the adhesive layer stress distribution for a single lap joint and Figure 8b shows the results for double lap joint. Table 2 shows the σ_{az} and τ_{ax} values obtained at the left edge of the adhesive layer for single and double lap joint (Fig. 1). Based on the results, it is observed that an increase in the overlap length leads decreases of stress state in the adhesive edge, mainly

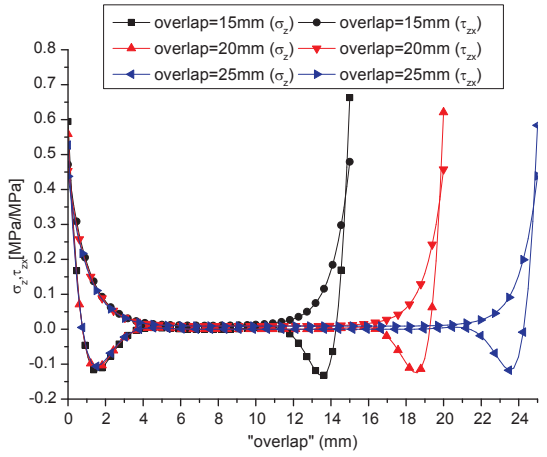

(a)

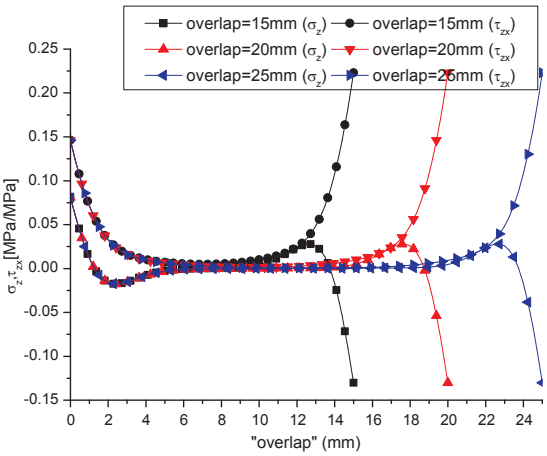

(b)

Figure 8. Overlap length: (a) single lap joint; (a) double lap joint.

Table 2. Normalized maximum absolute stress values for various overlap lengths at the left edge of the adhesive layer

Single lap joint			
Overlap length (mm)	15	20	25
σ_{az}	0.663	0.621	0.583
τ_{ax}	0.479	0.457	0.439
Double lap joint			
Overlap length (mm)	15	20	25
σ_{az}	0.130	0.130	0.130
τ_{ax}	0.223	0.223	0.223

for single lap joints, considering the lengths studied in this paper. Besides, the rate for stress reduction decreases with an increase in the overlap length. So, it is possible to conclude that there is a length in which any further increases in the overlap length do not decrease the stress state in the adhesive layer edge. This trend is clearer for the double lap joint.

Comparison between single and double lap joints

For this study, all the joint parameters for single and double lap joint were kept the same as for the overlap effect analysis. It is important to note that the overlap length is equal 20 mm. The results are shown for half of the overlap length in the region with greater differences between these two types of joints.

Figure 8 shows the difference between double and single lap joint stress distribution in the adhesive layer for the same load conditions and same joint characteristics. Figure 9a shows the difference between these two types of bonded joints for shear stress in the zx-plane (τ_{ax}) and Fig. 9b shows the difference for the normal stress (σ_{az}). As expected, the amplitude range of σ_{az} and τ_{ax} values are significantly greater for single lap joints.

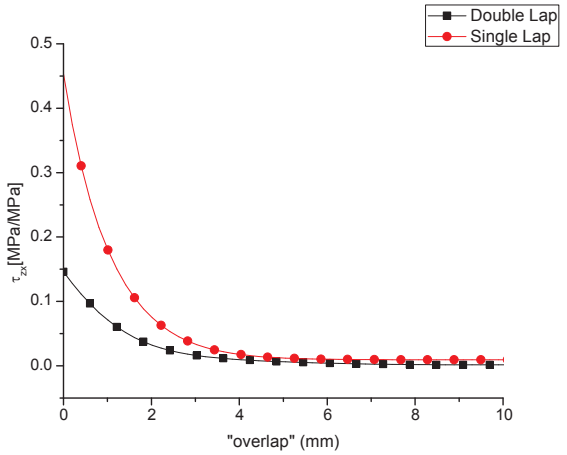

(a)

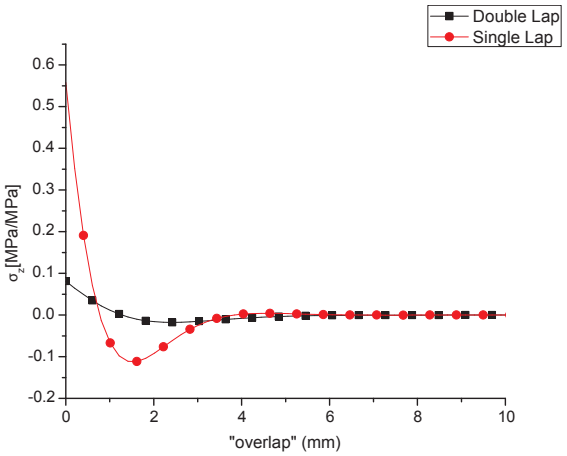

(b)

Figure 9. Single vs. double lap joint (half of the overlap length): (a) normalized τ_{zx} shear stress in plane *zx*; (b) normalized σ_z normal stress in *z* direction.

Effect of the adhesive elastic modulus

Another important parameter is the adhesive elastic modulus. This parameter was investigated, keeping other parameters constant and using three realistic values for the adhesive elastic modulus (1.5GPa; 2.0GPa; 3.0GPa) found in the literature (San Román, 2005).

Analysis of the effect of this parameter on the stress distribution in the adhesive layer was performed. In this case study, a normal load of 1 N/mm was imposed for both types of joints. Figure 10a shows the results for single lap joint, and Fig. 10b for double lap joint.

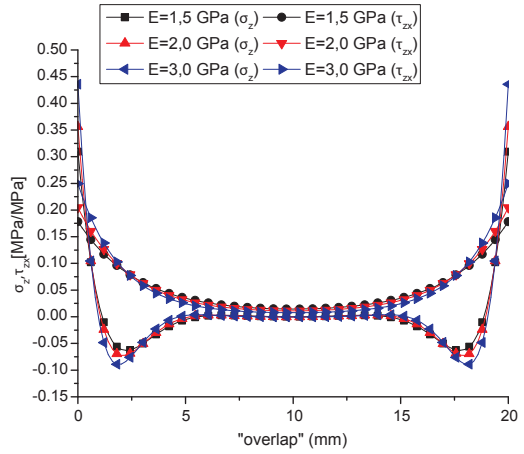

(a)

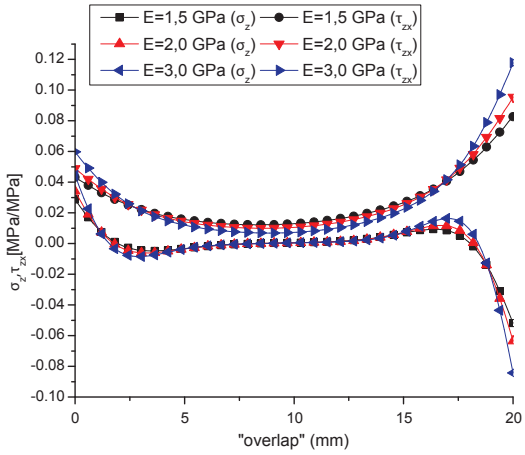

(b)

Figure 10. Young modulus: (a) single lap joint; (b) double lap joint.

It can be observed that adhesives with lower values of elastic modulus lead to lower stress state in the overlap region for single and for double lap bonded joints. This can be explained by Eqs. (4), (5) and (6). However, more flexible adhesives have low strength values, and in a real joint design, it is desirable that the adhesive has a satisfactory performance. Thus, it is important to balance the stiffness and the strength of the adhesive layer. Besides, the adhesive can show inelastic strains according to the level of loading and the yielding stress of the polymer.

Effect of the adhesive layer thickness

The adhesive layer thickness affects the stress distribution in the adhesive layer. This parameter was investigated, keeping the other parameters constant, regarding three realistic adhesive layer thicknesses (0.05 mm; 0.5 mm; 1.0 mm), which are found in the literature (Qian and Sun, 2009). The mechanical properties and composite adherents and adhesive characteristics are shown in Table 1. The analyses were carried out using a normal load of 1 N/mm. This load leads to adhesive stresses low enough to avoid adhesive non-linear behavior, or any adhesive or adherent failure.

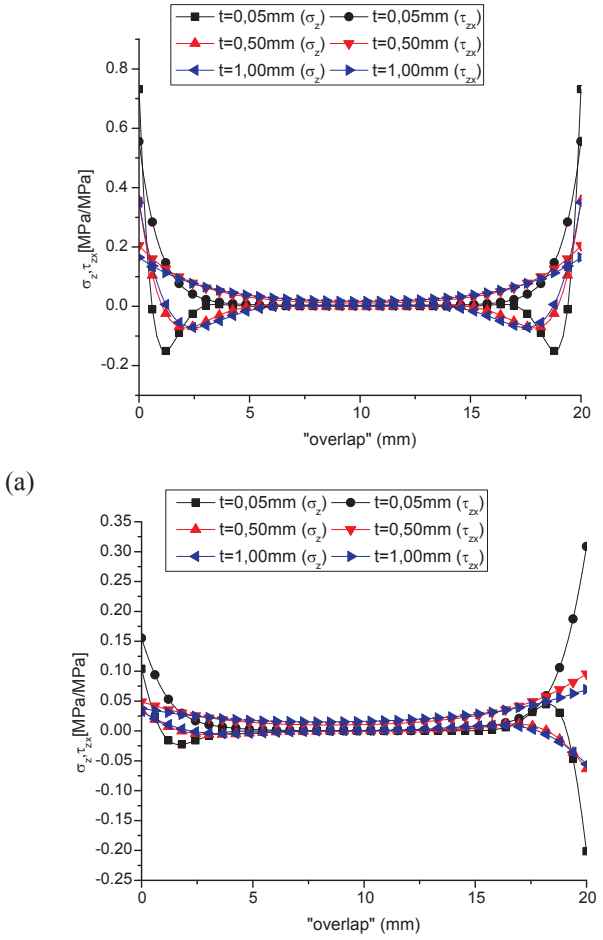

Figure 11.Adhesive thickness: (a) single lap joint; (b) double lap joint.

Figure 11a shows a single lap joint adhesive stresses distribution for three different thicknesses, and Fig. 11b for double lap joint. These results show that this parameter can significantly affect the adhesive layer stress distribution, mainly close to the edge of the overlap region. Adhesives with lower values of thickness lead to higher stress state in the overlap region for single and for double lap bonded joints. This can be explained by Eqs. 4, 5 and 6.

CONCLUSIONS

SAJ, a new computational tool, has shown to be adequate in performing composite-composite and metal-composite single and double bonded joint analysis. Therefore, very quickly, it is possible to analyze a set of different joints, varying many parameters, for example: materials (adhesives and/or adherents); fiber orientation and stacking sequence of the laminate; thickness of the laminate and/or the adhesive; overlap length and the type of the joint (single or double). However, due to the cylindrical flexural hypotheses, the computational tool provided some small deviations in the results, when compared to finite element analyses. In regards to stress distribution, SAJ resulting values are greater than finite element analyses. Thus, the analyses from SAJ are more conservative, which is very interesting for conceptual and preliminary design of a product.

Regarding to parametric study, SAJ leads to some conclusions, which can be used as a guide during product design. For example, a thicker adhesive layer (keeping other parameters constant) could reduce the adhesive edge stress state, increasing the strength of the joint, but thicker adhesives could lead to adhesive cohesive failure. The adhesive stiffness affects the stress state and a more flexible adhesive reduces the stress peak at the edges of the adhesive layer. Therefore, it is more recommendable to use more flexible adhesives. However, more flexible adhesives normally have lower strength values. Thus, it is important to verify what is more important to the product in service. Short overlap length increases the stress peak at the adhesive layer edges. Thus, it is reasonable to increase the overlap length, but the joint weight could increase too. Therefore, it is very important to balance all parameter values. Finally, by understanding the behavior of the stress distribution in the joint, it is possible to design products made of bonded joints with more accuracy even during the conceptual and preliminary phases.

REFERENCES

Agnieszka, D., 2009, "Prediction of the failure metal-composite bonded joints", Computational Materials Science, Vol. 45, No. 3, pp. 735-738.

Belhouari, M. *et al.*, 2004, "Comparison of double and single bonded repairs to symmetric composite structures: a numerical analysis", Composite Structures, Vol. 65, No. 1, pp. 47-53.

Butcher, J.C., 2003, "Numerical Methods for Ordinary Differential Equations", New York, John Wiley & Sons.

Charalambides, M.N. *et al.*, 1998, "Adhesively bonded repairs to fibre composite materials II: Finite elements modeling", Composites – Part A, Vol. 29, pp. 1383-1396.

Frostig, Y. *et al.*, 1997, "Analysis of adhesive bonded joints, square-end and spew-fillet: closed-form higher-order theory approach", Report No. 81, Institute of Mechanica1 Engineering, Aalborg University, Denmark.

Ganesh, V.K. and Choo, T.S., 2002, "Modulus graded composite adherents for single lap bonded joints", Journal of Composite Materials, Vol. 36, pp. 1757-1767.

Goland, M. and Reissner, E., 1944, "The stresses in cemented joints", Archive of Applied Mechanics. Vol. 11, pp. A17-A22.

Goyal, V.K. *et al.*, 2008, "Predictive strength-fracture model for composite bonded joints", Composite Structures, Vol. 82, No. 3, pp. 434-446.

Hart-Smith, L.J., 1973, "Adhesive-bonded scarf and stepped joints". Washington, DC, NASA, (NASA CR11223).

Hart-Smith, L.J., 1970, "The strength of adhesive-bonded single-lap joints", Santa Monica, Douglas Aircraft Company, IRAD Technical Report Number MDC-J0742.

Kim, T.H. *et al.*, 2008, "An experimental study on the effect of overlap length on the failure of composite to aluminum single lap bonded joints", Journal of Reinforced Plastic and Composites, Vol. 27, No.10, pp. 1071-1081.

Mortensen, F., 1998, "Development of Tools for Engineering Analysis and Design of High-Performance FRP-Composite Structural Elements". Ph.D. Thesis, Institute of Mechanical Engineering, Aalborg University, Aalborg.

Qian, H. and Sun, C.T., 2009, "Effect of bondline thickness on model I fracture in adhesive joints" in SDM 2008: Proceedings of the 49rd AIAA/ASME/ASCE/AHS/ASC Structures, Structural Dynamics, and Materials Conference, Schaumburg, Illinois, USA.

Ribeiro, M.L. *et al.*, 2010, "Development of a computational tool for bonded joint analysis" in PACAM XI: Proceedings of the 11th Pan-American Congress of Applied Mechanics, Foz do Iguaçu, Brazil.

Saha, G. and Banu, S. (2007), "Buckling load of a beam-column for different end conditions using multi-segment integration technique", Journal of Engineering and Applied Sciences, Vol. 2, No. 1, pp. 27-32.

San Román, J.C., 2005, "Experiments on epoxy, polyurethane and adhesives", Composite Structure Laboratory, Technical Report, CCLab2000.1b/1, Lausanne, Swiss.

Seong, M.S. *et al.*, 2008, "A parametric study on the failure of bonded single-lap joints of carbon composite and aluminum", Composite Structures, Vol. 86, pp. 135-145.

Shampine L. *et al.*, 2006, Solving Boundary Value Problems for Ordinary Differential Equations in MATLAB with bvp4c. ACM Transactions on Mathematical Software, Vol. 31, No. 1, pp. 79-94.

Silva, L.F.M. *et al.*, 2009a, "Analytical models of adhesively bonded joints-Part I: Literature survey", International Journal of Adhesion & Adhesives, Vol. 29, pp. 319-330.

Silva, L.F.M. *et al.*, 2009b, "Analytical models of adhesively bonded joints-Part II: Comparative study", International Journal of Adhesion & Adhesives, Vol. 29, pp. 331-341.

Springer, G.S. and Ahn, S.H., 1998, "Repair of composite laminates – II: models", Journal of Composite Materials, Vol. 32, No. 11, pp. 1076-1114.

Thomsen, O.T., 1992, "Elasto-static and elasto-plastic stress analysis of adhesive bonded tubular lap joints", Composite Structures, Vol. 21, pp. 249-259.

Tita, V. *et al.*,2008, Failure analysis of low velocity impact on thin composite laminates: Experimental and numerical approaches. Composite Structures, v. 83, pp. 413-428.

Xiaocong, H., 2011, "A review of finite element analysis of adhesively bonded joints", International Journal of Adhesion and Adhesives, Vol. 31, No. 4, pp. 248-264.

Yuceoglu, U. and Updike, D.P., 1975, "The effect of bending on the stresses in adhesive joints", Lehigh University, Bethlehem, Pensylvania (NASA).

Zarpelon, F.L., 2008, "Evaluation of Analytical Models for Bonded Repairs of Laminate Composite". Dissertation, Technological Institute of Aeronautics, São José dos Campos, Brazil (in Portuguese).

APPENDIX I

For Multiple Point Segment Method, consider the linear differential equations system in matrix notation

$$\frac{d}{dx}[y(x)] = A(x)\cdot y(x) + B(x) \tag{7}$$

Where: $y(x) = \begin{bmatrix} y_1 \\ y_2 \\ \cdots \\ y_m \end{bmatrix}$ (8)

$$A = \begin{bmatrix} a_{11} & a_{12} & \cdots & a_{1m} \\ a_{21} & a_{22} & \cdots & a_{2m} \\ \cdots & \cdots & \cdots & \cdots \\ a_{m1} & a_{m2} & \cdots & a_{mm} \end{bmatrix}, \quad B = \begin{bmatrix} b_1 \\ b_2 \\ \cdots \\ b_m \end{bmatrix} \tag{9}$$

The boundary conditions could be described as:

$$Cy(a) + Dy(b) = E \tag{10}$$

The solution can be regarded as:

$$y(x) = Y(x)\cdot G + Z(x) \tag{11}$$

Where: G is the integration constant, $Y(x)$ is the general solution of the system and $Z(x)$ is the particular solution.
Consider:

$$\frac{d}{dx}[Y(x)] = A(x).Y(x) \quad \text{with } Y(a) = I \tag{12}$$

$$\frac{d}{dx}[Z(x)] = A(x)\cdot Z(x) + B(x) \quad \text{with } Z(a) = 0 \tag{13}$$

Solving the equation in x = a:

$$y(a) = Y(a)\cdot G + Z(a). \tag{14}$$

Solving equation 14 in $x=a$, yield $G=Y(a)$ and for $x=b$. Applying this results in (10), yields

$$y(a) = [C + D\cdot Y(b)]^{-1}\cdot[E - D\cdot Z(b)] \tag{15}$$

Saha and Banu (2007) showed other example of the multiple point segment method application.

APPENDIX II

For the Matlab function "bvp4c", consider a differential equation $y''+ y = 0$ smooth in the [a,b]. The boundary condition in $x = a$ is $y(a) = A$ and $y'(a) = s$, the solution of the differential equation have to find the value of $y(b,s) = B$.

Consider that the algebraic equation s has a solution. Regard a function *u(x)* as the solution for $y(a) = A$ and $y'(a) = 0$ and *v(x)* be the solution for $y(a) = 0$ and $y'(a) = 1$, this linear approach yields in $y(x,s) = u(x) + sv(x)$ and with the boundary condition $B = y(b,s) = u(b) + sv(b)$, its results in a linear set of algebraic linear equations with initial derivative equal s.

In some kind of problems, the equations to solve the problem are non-linear. It implies that the existence and the uniqueness of the results are very difficult problem to solve.

In practice, to solve a set of differential non-linear equations are based in the solution of initial value problem and in non-linear equations solvers. Matlab™ "bvp4c" function uses the colocation method to solve the problem. For example, consider the following differential equation:

$$y' = f(x,y,p), \quad a \le x \le b \tag{16}$$

And the non-linear boundary conditions in x = a and x = b are:

$$g(y(a),y(b),p) = 0 \tag{17}$$

Where p is the vector of unknown parameters. The approximate solution, S(x), is a third order polynomial function smooth in the interval $[x_n, x_{n+1}]$ with mesh $a = x_0 < x_1 < \ldots < x_n < b$, satisfying the boundary condition $g(S(a), S(b)) = 0$ the interval limits as well as the differential equations inside the mesh.

$$\begin{aligned} &S'(x_n) = f(x_n, S(x_n)) \\ &S'\left(\frac{x_n + x_{n+1}}{2}\right) = f\left(\frac{x_n + x_{n+1}}{2}, S\left(\frac{x_n + x_{n+1}}{2}\right)\right) \\ &S'(x_{n+1}) = f(x_{n+1}, S(x_{n+1})) \end{aligned} \tag{18}$$

This results in a non-linear system for $S(x)$.